ELSEVIER

Catalysis Today 72 (2002) 123–132

CATALYSIS TODAY

www.elsevier.com/locate/cattod

Oxidation of CO over Au/MO_x/Al_2O_3 multi-component catalysts in a hydrogen-rich environment

R.J.H. Grisel[a], C.J. Weststrate[a], A. Goossens[b], M.W.J. Crajé[c], A.M. van der Kraan[c], B.E. Nieuwenhuys[a,*]

[a] *Gorlaeus Laboratoria, Department of Heterogeneous Catalysis and Surface Chemistry, Leiden Institute of Chemistry, PO Box 9502, 2300 RA Leiden, The Netherlands*

[b] *Kamerlingh Onnes Laboratorium, Leiden University, PO Box 9504, 2300 RA Leiden, The Netherlands*

[c] *Interfacultair Reactor Institute, Delft University of Technology, Mekelweg 15, 2629 JB Delft, The Netherlands*

Abstract

Au/MgO/Al_2O_3 is able to oxidize CO selectively in hydrogen-rich gases (~70 vol.%) at the temperatures relevant to hydrogen fuel cell applications (70–100 °C). The presence of MgO enables the preparation of small, stable Au particles on γ-Al_2O_3 with high surface area and, in this way, improves both low-temperature CO and H_2 oxidation by O_2 compared to Au/Al_2O_3. Addition of MnO_x and FeO_x to Au/MgO/Al_2O_3 further enhances low-temperature CO oxidation with improved CO_2 selectivity. The increase in CO oxidation activity is attributed to the implementation of new routes for supplying active oxygen, e.g., via lattice oxygen. The better CO_2 selectivity also probably results from suppression of H_2 oxidation at low temperatures. The results support a model in which CO is adsorbed onto metallic Au or at the Au/MO_x perimeter interface and reacts with oxygen also present at the Au/MO_x perimeter interface. A focus on decreasing the H_2 oxidation activity is recommended for further catalyst improvement. © 2002 Elsevier Science B.V. All rights reserved.

Keywords: CO (selective) oxidation; H_2; Gold; Metal oxides; Alumina; Promoter effect; MnO_x; FeO_x; MgO

1. Introduction

With the knowledge that supported Au catalysts have high activity in low-temperature CO oxidation [1,2], new studies were focused on the activity of supported Au in various other oxidation reactions [3,4]. Although the nature of the active sites remains unclear, it is generally accepted that the presence of small Au particles highly dispersed on a suitable metal oxide (MO_x) is required to obtain high catalytic activity [1–5]. The high activity is attributed to (i) specific sites present on small metallic particles, such as coordinatively unsaturated Au surface atoms [6], (ii) small metallic particles with an altered electronic structure [7] and (iii) the presence of ionic/oxidic Au [8]. The role of MO_x is also still under discussion. While MO_x prevents small Au particles from sintering under mild conditions [9], it has been put forward that the Au/MO_x perimeter, defined as the boundary between Au, MO_x, and the gas phase, may be crucial for O_2 activation [10,11]. It has also been suggested that the reaction solely takes place on the Au/MO_x perimeter with CO adsorbed on Au and oxygen originating from MO_x [9,12].

---

[*] Corresponding author.
E-mail address: nieuwe_b@chem.leidenuniv.nl (B.E. Nieuwenhuys).

PII: S0920-5861(01)00486-2

In contrast to unsupported Au [13], supported Au is more active in CO oxidation than in the oxidation of H_2 [1,5,14]. This quite unique ability is employed in the present study in order to put together a highly reactive and selective catalyst for CO oxidation in the presence of H_2. The catalysts used include Au on MgO/Al_2O_3 and Au–MO_x on MgO/Al_2O_3 (M = Mn, Fe). We tried to elucidate the role of Au and MO_x in CO selective oxidation. The effects of the Au particle size and the presence of MO_x on the activity and the selectivity will be discussed. On the basis of our results we propose a formulation of a novel catalyst for the selective oxidation of CO. In addition, a mechanism is proposed for the relevant processes.

2. Experimental

2.1. Catalyst preparation

The catalytic activity of Au-based catalysts depends on the presence of small Au clusters. Earlier studies indicated that deposition of Au on $MgO/\gamma\text{-}Al_2O_3$ (5 wt.%, Au:Mg = 1:5) via homogeneous deposition precipitation resulted in a catalyst with a high surface area ($\sim$200 $m^2\,g^{-1}$) and very small Au particles, which was extremely active in CO (selective) oxidation [15]. Generally, the CO oxidation activity can be improved by adding MO_x [9,16]. Amongst the most effective additives are MnO_x and FeO_x. MO_x was applied onto 5 wt.% Au on MgO/Al_2O_3, yielding catalysts with an Au:Mg:M atomic ratio of 1:5:5. Details of the preparation are given elsewhere [15].

2.2. Catalyst characterization

The catalysts were examined in detail with high-resolution transmission electron microscopy (HRTEM) using a Philips CM30T electron microscope. The energy of the electrons used was 300 kV (resolution: $\sim$0.5 nm at 500 k magnification). Elemental analysis was possible by means of a built-in LINK EDX system. From each catalyst about 300 Au particles were measured in order to obtain a statistically justified particle size distribution.

To gather information on the chemical state of Au present on $Au/MgO/Al_2O_3$ and $Au/MnO_x/MgO/Al_2O_3$ catalysts, X-ray photoelectron spectroscopy (XPS) measurements were performed. The powdered samples were pressed onto a special sample holder, which was then placed in a vacuum chamber (base pressure $<10^{-7}$ mbar). A VG X-ray source with an aluminium crystal, operating at 10–15 kV anode voltage, 5 A filament current and 40 mA emission current, was used to generate the required Al Kα radiation (resolution: $\sim$0.8 eV).

^{197}Au-Mössbauer effect spectroscopy (MES) was applied to examine the electronic structure of Au in $Au/MgO/Al_2O_3$ and $Au/MnO_x/MgO/Al_2O_3$. The results were compared to Au/Al_2O_3 with similar Au particle size. The spectra were obtained using ^{197}Pt in a Pt source prepared by thermal neutron (n) bombardment of ^{196}Pt enriched Pt powder for 24 h, which resulted in a 200 MBq Mössbauer source. The transmitted ^{197}Au γ-rays were detected with a high purity Ge detector. During measurement the absorbers and source were kept at 4.2 K. All spectra have been analysed using as few subspectra as possible.

2.3. Activity measurements

The oxidations were carried out in a lab-scale flow reactor. Before measurement, the catalysts were reduced in situ in an atmosphere of 4 vol.% H_2 (balance He) at 300 °C (heating rate 10 °C min^{-1}) and kept at 300 °C for 30 min. The reactor was cooled to room temperature (RT) before introducing the reactant flow (40 ml min^{-1}, GHSV $\sim$2500 h^{-1}). Reactions were performed in a mixture of H_2 ($\sim$70 vol.%), He ($\sim$29 vol.%) and O_2 + CO (1.2 vol.%) with varying O_2:CO molar ratio ($\lambda = 1, 2, 4$). The parameter λ is defined as the amount of O_2 present divided by the amount of O_2 needed to completely oxidize all the CO in the feed [17]. After stabilization at RT for 30 min, three cycles of heating and cooling curves were recorded consecutively to monitor possible hysteresis and catalyst (de)activation. After the last cooling stage, the catalyst was kept at RT for an extended period of time ($\sim$9 h) to evaluate the activity and selectivity in time on stream. On-line gas analysis was performed by a Balzers QMG-064 mass spectrometer and a Chrompack CP 2002 gas chromatograph equipped with a Molsieve 5 Å column for CO and O_2 detection and a Hayesep A column for CO_2 detection.

Table 1
Catalyst characterization (HRTEM, XPS, ^{197}Au-MES)

Catalyst	HRTEM	XPS		MES (non-bulk)	
	Au diameter (nm)	$4f_{7/2}$ (eV)	$4f_{5/2}$ (eV)	IS ($mm\,s^{-1}$)	QS ($mm\,s^{-1}$)
Au/Al_2O_3	3.6 ± 1.4	83.7	87.3	−0.63	1.45
$Au/MgO/Al_2O_3$	2.6 ± 1.0	83.8	87.4	−1.15	4.10
				−0.98	1.41
$Au/MnO_x/Al_2O_3$	4.2 ± 1.1	83.7	87.3	−0.84	2.18
$Au/MnO_x/MgO/Al_2O_3$ dried at 80 °C, >16 h	–	–	–	2.67	3.92
				3.70	4.59
$Au/MnO_x/MgO/Al_2O_3$ calcined at 300 °C, 2 h	2.5 ± 1.2	83.5	87.3	−1.45	3.27
				0.29	5.16
$Au/FeO_x/MgO/Al_2O_3$	3.2 ± 1.4	–	–	–	–

3. Results

3.1. Catalyst characterization

The average Au particle sizes of the catalysts are summarized in Table 1. Au/Al_2O_3 is given as reference. HRTEM–EDX studies indicate that the MgO and FeO_x phases are most probably well-dispersed, whereas MnO_x is less homogeneously dispersed. No traces of Cl^- or other contaminants were found. Lattice spacings, occasionally observed for small Au particles, indicate the presence of metallic Au ($d = 2.355$ Å). Nonetheless, based on these results only it cannot be concluded a priori that no oxidic Au is present.

XPS spectra of Au/Al_2O_3 (reference), $Au/MgO/Al_2O_3$ and $Au/MnO_x/MgO/Al_2O_3$ are given in Fig. 1. All spectra could be fitted satisfactorily with peak maxima at 87.3 and 83.7 eV binding energy, which are characteristic of metallic Au. No $Au^{\delta+}$ was detected. It must be noted, however, that the apparatus used has a low response and is probably not sensitive to the presence of very small amounts of oxidic Au.

Fig. 2A shows MES spectra of the same catalysts. All ^{197}Au spectra consist of a clear bulk Au peak and a small surface contribution. The isomer shift (IS) of metallic Au was constrained to $-1.22\,mm\,s^{-1}$. The surface contributions were best fitted with doublets; the quadrupole splitting (QS) values depending on the symmetry of the local coordination of the surface atoms. Because of the slight asymmetry in the spectra for $Au/MgO/Al_2O_3$ and $Au/MnO_x/MgO/Al_2O_3$ more doublets were needed to fit the data satisfactorily. The ^{197}Au spectra of $HAuCl_4{\cdot}3H_2O$ and uncalcined $Au/MnO_x/MgO/Al_2O_3$ are shown in Fig. 2B. After washing and drying the catalyst at 80 °C no evidence of starting material was found. A high intensity doublet with a large positive IS indicates that besides metallic Au another Au species, possibly $Au(OH)_3$, is present on the catalyst. After calcination in O_2 at 100 °C for 30 min (not shown) no changes have been observed. Catalyst pretreatment at higher temperatures did alter the chemical properties of the Au phase. After calcination at 300 °C (Fig. 2A, curve c) a negative IS was observed. The results are summarized in Table 1. Mössbauer measurements on different Au compounds have led to the identification of IS/QS combinations

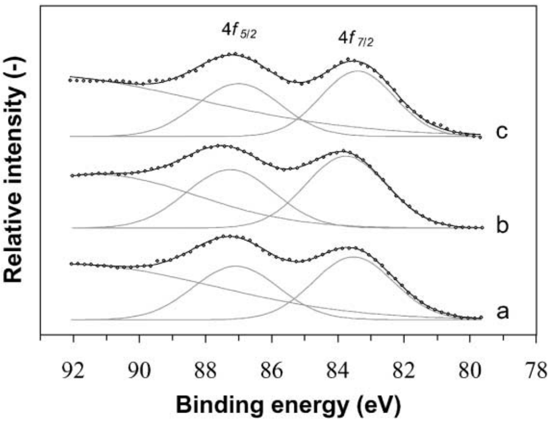

Fig. 1. The $4f_{7/2}$ and $4f_{5/2}$ electron binding energies of Au in Au/Al_2O_3 (a), $Au/MgO/Al_2O_3$ (b) and $Au/MnO_x/MgO/Al_2O_3$ (c). The O 1s peak (constrained to binding energy = 531.0 eV) was used as internal reference.

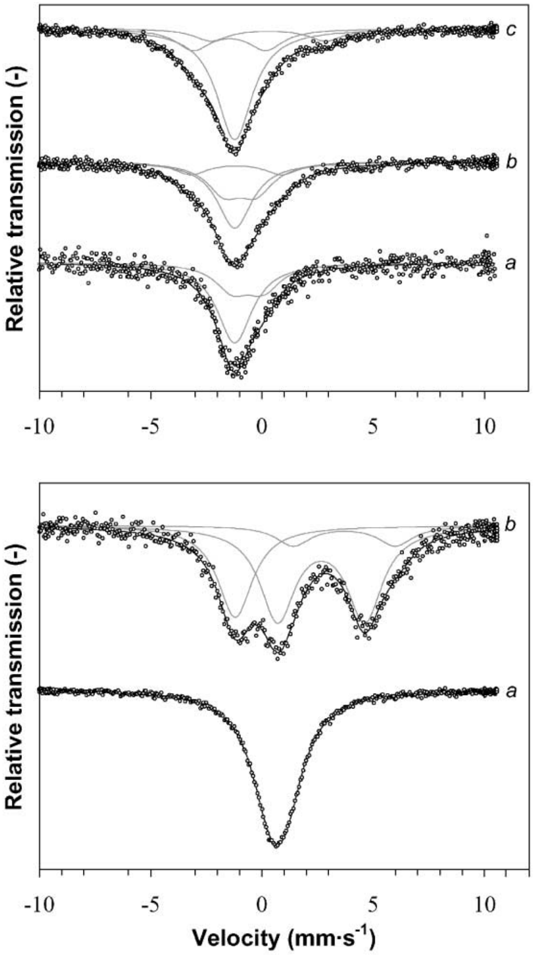

Fig. 2. Top: Mössbauer spectra for Au/Al_2O_3 (a), $Au/MgO/Al_2O_3$ (b) and $Au/MnO_x/MgO/Al_2O_3$ (c) calcined at 300 °C for 2 h. Bottom: Mössbauer spectra for $HAuCl_4{\cdot}3H_2O$ (a) and $Au/MnO_x/MgO/Al_2O_3$ dried at 80 °C for >16 h (b). Spectra relative to absolute velocity.

which are typical of Au^0, Au^I, Au^{III} and Au^V [18]. In order to identify the second Au species present on the catalysts studied, the IS values are plotted versus the QS in Fig. 3. For comparison spectra obtained for $HAuCl_4{\cdot}3H_2O$, $Au(OH)_3$, Au/Al_2O_3 and Au/MnO_x are shown also.

After reaction the catalysts were examined with XRD and HRTEM. Oxidation experiments did not influence the Au particle size (distribution) nor the catalyst morphology significantly.

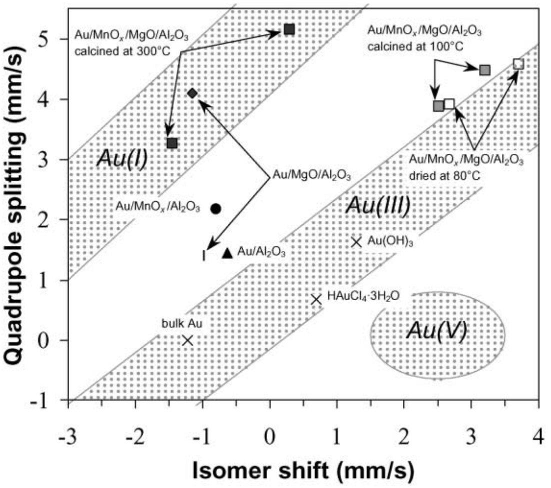

Fig. 3. IS vs. QS of non-bulk Au species extracted from Mössbauer spectra of the catalysts under study. Also shown are bulk (metallic) Au, $HAuCl_4{\cdot}3H_2O$, $Au(OH)_3$ and $Au/MnO_x/Al_2O_3$.

3.2. Activity measurements

The results of CO oxidation on $Au/MgO/Al_2O_3$ are presented in Fig. 4. The left-hand side of the figure depicts the CO conversion during three consecutive reaction cycles as a function of temperature. The right-hand side shows the same data for CO conversion, as well as O_2 conversion and the calculated selectivity, but here as a function of the total reaction time. In all cases almost all of the O_2 in the flow was consumed. Therefore, the CO_2 selectivity is practically similar to the CO conversion divided by λ. At high O_2:CO ratio ($\lambda = 4$) the system was not in quasi-steady state; the CO conversion (and selectivity) increased upon subsequent reaction cycles (Fig. 4a and b). However, during the first 3 h in time on stream at RT ($t = 7$–10 h) the CO conversion, and to a lesser extent the O_2 conversion, decreased, lowering the selectivity to CO_2, after which it reached steady state. Moreover, a large hysteresis was observed, in which the CO conversion in the cooling branches exceeded those of the heating branches at low temperatures (Fig. 4a). In addition, a maximum in CO conversion was found at 140–160 °C during the heating stages. Upon lowering the O_2:CO ratio ($\lambda = 2, 1$) the catalytic behaviour was similar throughout all reaction cycles. It was noted that differences in CO conversion

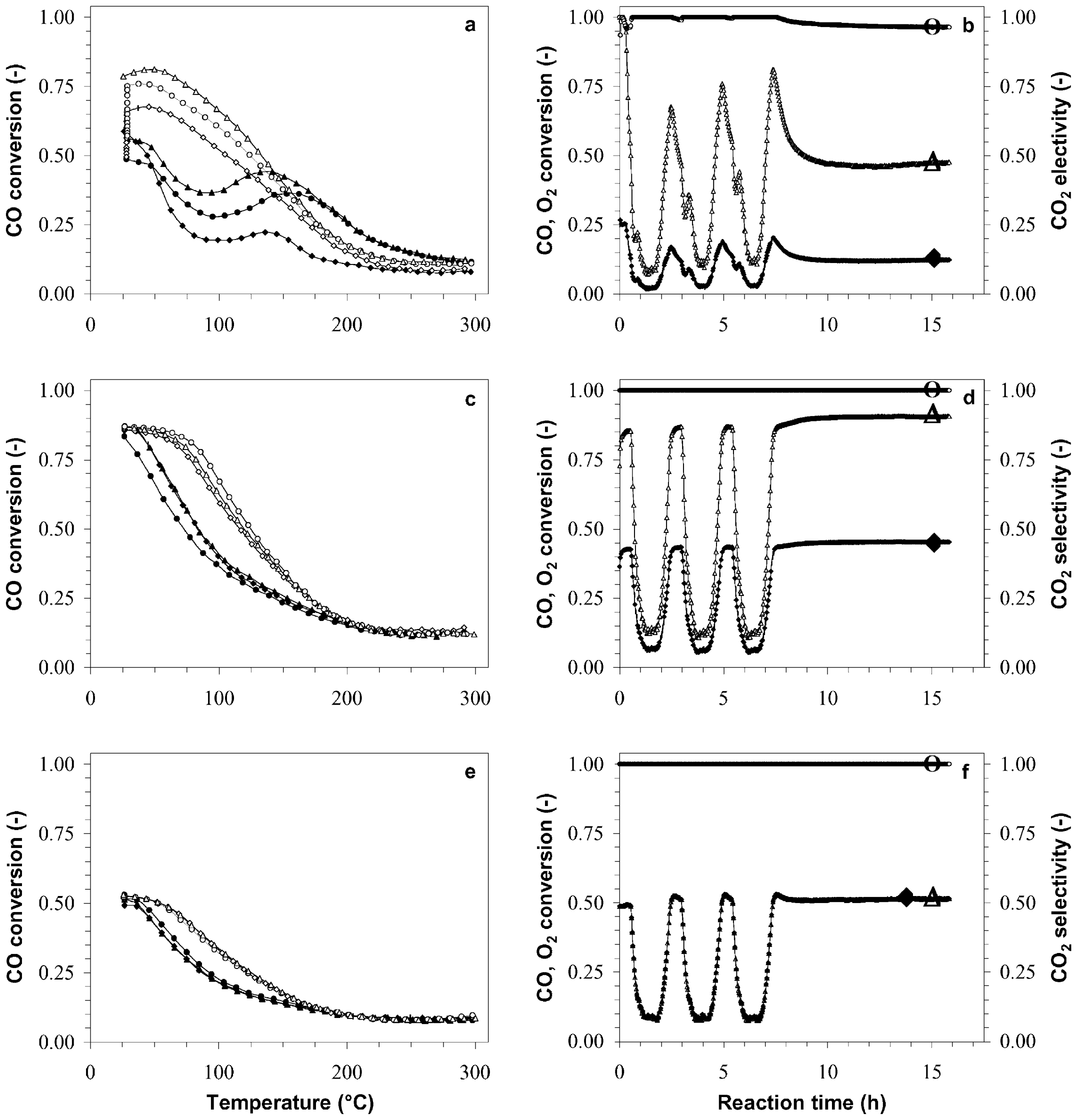

Fig. 4. Catalytic activity of $Au/MgO/Al_2O_3$. Left: heating (closed symbols) and cooling (open symbols) curves of CO conversion vs. temperature (°C); first (◆), second (●) and third (▲) reaction cycle. Right: conversion of CO (△) and O_2 (○), and the selectivity towards CO_2 (◆) vs. reaction time (h) for $\lambda = 4$ (a and b), 2 (c and d) and 1 (e and f).

during the heating and cooling stages decreased with lower λ-values. Although for $\lambda = 2$ and 1 initially a slight increase (Fig. 4d), respectively decrease (Fig. 4f) in CO conversion was observed, the CO_2 selectivity in time on stream at RT was stable for ~9 h.

Results of CO selective oxidation after adding MnO_x and FeO_x to $Au/MgO/Al_2O_3$ are shown in Figs. 5 and 6, respectively. Whereas MnO_x addition improved CO oxidation activity over the entire temperature range studied for all λ (Fig. 5), the effect of FeO_x is most pronounced at low temperatures (Fig. 6). The presence of MO_x typically reduced the hysteresis effect, especially for FeO_x at low λ. Similar to $Au/MgO/Al_2O_3$ for $\lambda = 4$ the O_2 conversion dropped at

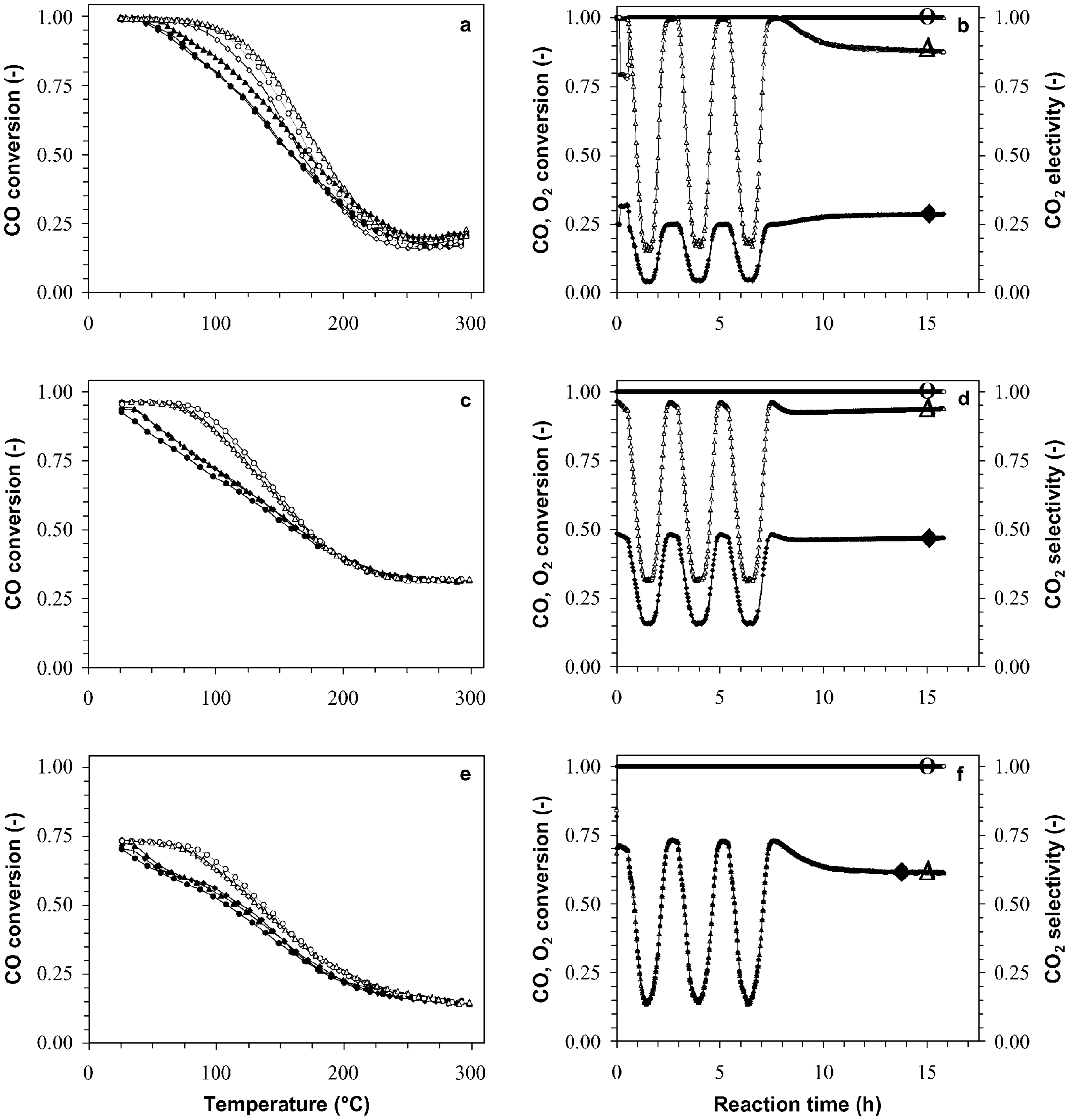

Fig. 5. Catalytic activity of Au/MnO$_x$/MgO/Al$_2$O$_3$. Left: heating (closed symbols) and cooling (open symbols) curves of CO conversion vs. temperature (°C); first (◆), second (●) and third (▲) reaction cycle. Right: conversion of CO (△) and O$_2$ (○), and the selectivity towards CO$_2$ (◆) vs. reaction time (h) for $\lambda = 4$ (a and b), 2 (c and d) and 1 (e and f).

RT in time on stream for both Au/MnO$_x$/MgO/Al$_2$O$_3$ (Fig. 5b) and Au/FeO$_x$/MgO/Al$_2$O$_3$ (Fig. 6b). However, since the CO conversion was unaffected on MnO$_x$ and decreased less than the O$_2$ conversion on FeO$_x$ comprising catalysts, the selectivity towards CO$_2$ increased, this in contrast with Au/MgO/Al$_2$O$_3$. The results are summarized in Table 2.

4. Discussion

4.1. Chemical state and role of Au

It is generally accepted that the low-temperature CO oxidation activity depends on the Au particle size [1–5]. Other studies also indicate a particle size

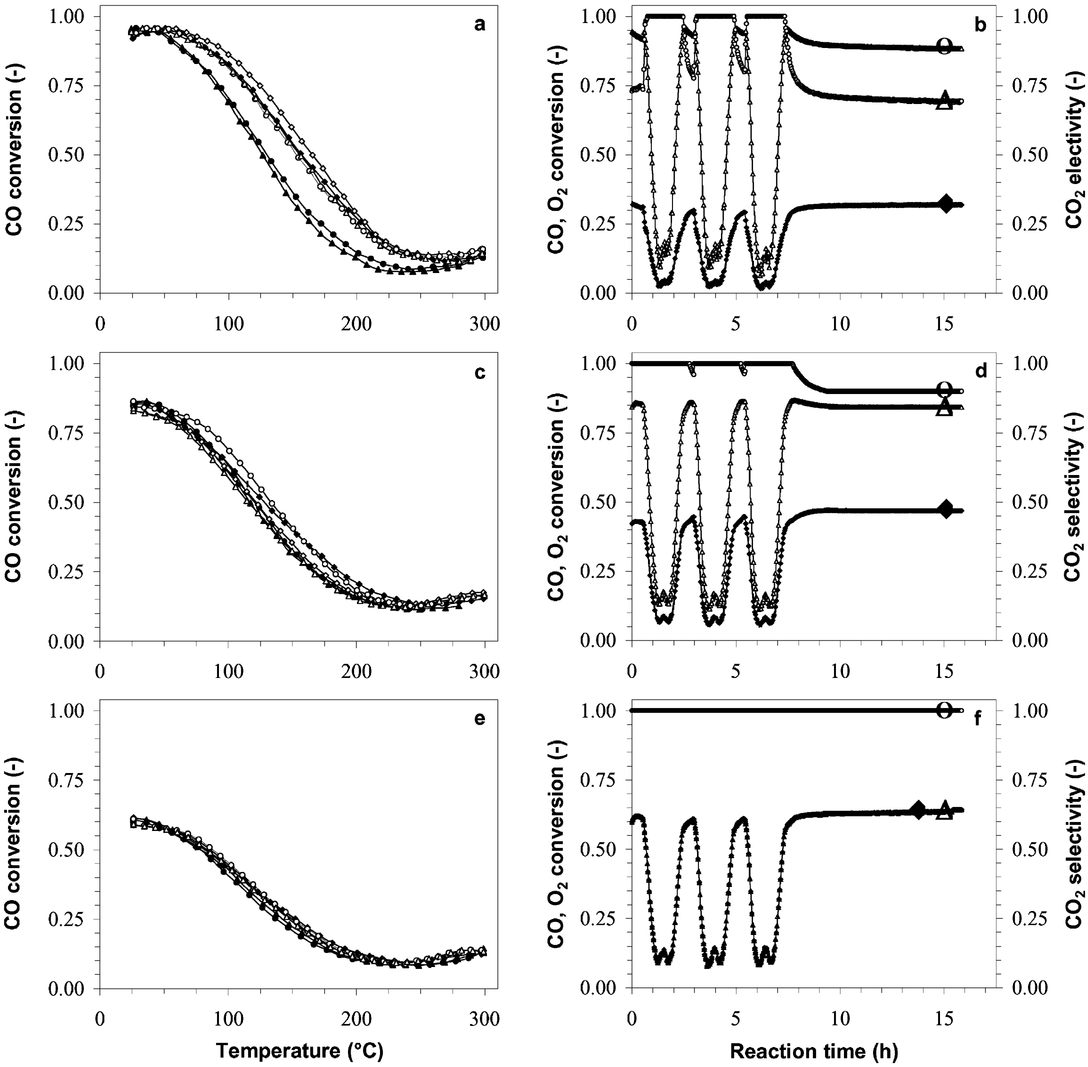

Fig. 6. Catalytic activity of Au/FeO$_x$/MgO/Al$_2$O$_3$. Left: heating (closed symbols) and cooling (open symbols) curves of CO conversion vs. temperature (°C); first (◆), second (●) and third (▲) reaction cycle. Right: conversion of CO (△) and O$_2$ (○), and the selectivity towards CO$_2$ (◆) vs. reaction time (h) for $\lambda = 4$ (a and b), 2 (c and d) and 1 (e and f).

effect for CH_4 oxidation on Au/Al_2O_3, in which small Au particles are beneficial for high activity [19]. It was concluded that small, most probably metallic, Au particles are capable of C–H bond activation. Exploratory studies on CO oxidation in the presence of H_2 also show the necessity of the presence of small Au particles [15].

No direct evidence for oxidic/ionic Au species was found. From the literature [20] and extrapolation of MES data in this study one might argue about the existence of Au^I species in Mg comprising Au-based catalysts (Fig. 3). However, since the data were fitted with as few subspectra as possible while we did not know the actual number of different surface Au species, these results have no real physical meaning. More extensive investigations are necessary to draw firm conclusions from these measurements. In addition, no clear correlation was found between the

Table 2
CO conversion and selectivity to CO_2 during 3rd reaction cycle at 70 °C

Catalyst	CO conversion			CO_2 selectivity		
	$\lambda = 4$	$\lambda = 2$	$\lambda = 1$	$\lambda = 4$	$\lambda = 2$	$\lambda = 1$
Heating						
$Au/MgO/Al_2O_3$	0.40	0.60	0.32	0.10	0.30	0.32
$Au/MnO_x/MgO/Al_2O_3$	0.94	0.82	0.61	0.24	0.41	0.61
$Au/FeO_x/MgO/Al_2O_3$	0.87	0.75	0.54	0.22	0.37	0.54
Cooling						
$Au/MgO/Al_2O_3$	0.77	0.81	0.45	0.19	0.40	0.45
$Au/MnO_x/MgO/Al_2O_3$	0.99	0.95	0.72	0.25	0.47	0.72
$Au/FeO_x/MgO/Al_2O_3$	0.91	0.74	0.54	0.23	0.37	0.54

possible presence of such Au species and the catalytic activity. Previous activity measurements and FTIR studies indicate that reduced Au-based catalysts are superior to oxidized ones in low-temperature CO oxidation [15,16]. Moreover, the CH_4 oxidation activity observed for Au-based catalysts at temperatures well above the decomposition temperature of AuO_x does not plead for the presence of oxidic Au [19], at least at these temperatures. Therefore, we suggest that Au^I species, if present, are not necessary to obtain high catalytic activity. The primary role of Au is thought to be the adsorption of CO, but it may also assist oxygen activation at the Au/MO_x perimeter interface via surface OH groups [21] or via O-vacancies in the MO_x lattice [9,15,16].

4.2. Effect of MO_x

Previous studies indicated that the effect of MO_x may be twofold. On the one hand, it may prevent small Au particles on Al_2O_3 from sintering to a certain extent even up to temperatures above 700 °C [9,15], probably due to encapsulation of the Au particles. Of the MO_x studied, MgO was found to have the largest stabilizing effect on the Au particle size. In addition to the effect on the Au particle size the presence of MO_x can have a direct impact on the catalytic activity [9,15,16]. An improved activity was found for types of M that can easily change their valency (M = Mn, Fe and Co).

Our results show that addition of MnO_x and FeO_x to $Au/MgO/Al_2O_3$ leads to improved CO oxidation activity in H_2 rich gas (70 vol.%), but does not perceptibly affect the chemical and physical state of the Au phase. Also, large differences in CO_2 selectivity were found. This is directly related to the overall changes in the CO and H_2 oxidation activity. It is thought that lattice oxygen [15,16] and surface OH groups on MO_x [21] may be crucial to obtain high catalytic activity. Introduction of MnO_x and FeO_x thus enables an extra route for the supply of active oxygen, but it may also partially block sites on $Au/MgO/Al_2O_3$ which are highly reactive towards H_2 oxidation, both leading to improved CO_2 selectivity.

4.3. Model for CO selective oxidation over $Au/MO_x/MgO/Al_2O_3$

Lower λ-values decrease the low-temperature CO oxidation activity. On the other hand, the selectivity to CO_2 increases since the fraction of O_2 used to oxidize H_2 also decreases. Moreover, differences in CO conversion during the heating and cooling stages become smaller. This hysteresis in rate is typical of H_2 oxidation on highly active Au catalysts [15]. It was suggested that H_2O accumulation on the catalyst at low temperature is responsible for the lower activity observed during the heating stage. The hysteresis becomes smaller upon CO addition (H_2:CO:O_2 = 4:2:1). A possible explanation is that CO can block sites needed for H_2 activation at low temperatures, thus preventing the formation of large amounts of H_2O. With excess of H_2 (70 vol.%) a certain fraction of H_2 will be oxidized, resulting in built-up of water and, accordingly, hysteresis (Section 3.2). In this view a lower λ would result in less H_2O formation and, hence, in a smaller difference in CO conversion during heating and cooling stages, as was observed in our experiments. Addition of MnO_x (Fig. 5) and especially FeO_x (Fig. 6) was found to reduce hysteresis in CO conversion for all O_2:CO ratios studied. The addition of MnO_x to $Au/MgO/Al_2O_3$ increases the CO oxidation and reduces the H_2 oxidation activity [15]. The same may hold for FeO_x.

Based on the results described in this paper as well as those obtained from previous studies [9,15,16], we propose the following mechanism for the oxidation of CO in a hydrogen atmosphere. CO is adsorbed on small, mainly metallic, Au particles and at the Au/MO_x perimeter. H_2 adsorption is partly blocked at low temperature (<100 °C) because of CO interference. At higher temperatures the CO desorption rate increases allowing more H_2 to reach the surface and react, resulting in a decrease in selectivity. An increase in λ, i.e. upon lowering the CO partial pressure, may induce a similar effect. Active oxygen may originate from the lattice of MO_x or from activated oxygen at the Au/MO_x perimeter interface or at surface OH groups [21] in the vicinity of small Au particles. The reaction most likely occurs at the Au/MO_x perimeter interface.

Regarding possible applications in PEFC technology both a high CO conversion and a high selectivity towards CO_2 (at 70–100 °C) are crucial. However, due to the poisoning effect of CO a near 100% conversion is desirable. Within these restrictions the best results were found for $Au/MnO_x/MgO/Al_2O_3$ ($\lambda = 2, 4$) and $Au/FeO_x/MgO/Al_2O_3$ ($\lambda = 4$). Excess of O_2 is needed to obtain high CO conversion in the relevant temperature range, at the expense of CO_2 selectivity. Since $Au/MO_x/Al_2O_3$ (M = Mg, Mn, Fe, Ni and Zn) are able to oxidize CO completely under the working conditions of hydrogen-based fuel cells [9,15], the emphasis should now be laid on increasing the CO_2 selectivity, i.e. lowering the H_2 oxidation activity. Therefore, MgO may not be the most ideal Au particle size stabilizer, since $Au/MgO/Al_2O_3$ is the most active catalyst in H_2 oxidation [15].

5. Conclusions

Au/Al_2O_3 is able to oxidize CO in hydrogen-rich gases (~70 vol.%), provided that small Au particles are present. MgO addition enables the preparation of a reproducible, highly dispersed and thermally stable Au particles on Al_2O_3. Addition of MnO_x and FeO_x results in an increase in CO conversion, especially at low temperatures. In addition, the CO_2 selectivity benefits considerably from the presence of both oxides in the entire temperature range studied. Increasing the O_2:CO atomic ratio generally leads to a higher CO conversion, but a decrease in CO_2 selectivity.

The results fit a model in which CO and H_2 compete for adsorption sites on metallic Au or at the Au/MO_x perimeter, and oxygen originates from the lattice of the transition metal oxide in the vicinity of small Au particles or from activated oxygen at the Au/MO_x perimeter. At low temperatures (<100 °C) the relatively high abundance of adsorbed CO leads to high CO_2 selectivity. Higher temperatures and O_2 partial pressures decrease CO_2 selectivity due to higher H_2 oxidation rates.

Regarding possible application in hydrogen fuel cells, the best results were obtained for $Au/MnO_x/MgO/Al_2O_3$. Further research should focus on inhibition of the H_2 oxidation reaction rather than improving the CO oxidation activity.

Acknowledgements

The authors thank Dr. P.J. Kooyman of the National Centre for High Resolution Electron Microscopy, Delft University of Technology, Delft, The Netherlands, for performing the electron microscopy investigations. This work has been performed under auspices of NIOK, The Netherlands Institute for Catalysis Research. Lab Report # UL 01-2-02. Part of this work is supported by INTAS, reference number 99-01882.

References

[1] M. Haruta, N. Yamada, T. Kobayashi, S. Iijima, J. Catal. 115 (1989) 301.
[2] M. Haruta, S. Tsubota, T. Kobayashi, H. Kageyama, M. Genet, B. Delmon, J. Catal. 144 (1993) 175.
[3] M. Haruta, Catal. Today 36 (1997) 153.
[4] G.C. Bond, D.T. Thompson, Catal. Rev. Sci. Eng. 41 (1999) 319.
[5] M. Okumura, S. Nakamura, S. Tsubota, T. Nakamura, M. Azuma, M. Haruta, Catal. Lett. 51 (1998) 53.

[6] M.A.P. Dekkers, M.J. Lippits, B.E. Nieuwenhuys, Catal. Lett. 56 (1998) 195.
[7] Valden, X. Lai, D.W. Goodman, Science 281 (1998) 1647.
[8] S. Minicò, S. Scirè, A. Visco, S. Galvano, Catal. Lett. 47 (1997) 273.
[9] R.J.H. Grisel, B.E. Nieuwenhuys, Catal. Today 64 (2001) 69.
[10] G.R. Bamwenda, S. Tsubota, T. Nakamura, M. Haruta, Catal. Lett. 44 (1997) 83.
[11] S. Tsubota, T. Nakamura, K. Tanaka, M. Haruta, Catal. Lett. 56 (1998) 131.
[12] B.E. Nieuwenhuys, in: R.W. Joyner, R.A. van Santen (Eds.), Elementary Reaction Steps in Heterogeneous Catalysis, Kluwer Academic Publishers, Dordrecht, 1993.
[13] Y. Iizuka, H. Fujiki, N. Yamauchi, T. Chijiiwa, S. Arai, S. Tsubota, M. Haruta, Catal. Today 36 (1997) 115.
[14] R.M. Torres Sanchez, A. Ueda, K. Tanaka, M. Haruta, J. Catal. 168 (1997) 125.
[15] R.J.H. Grisel, B.E. Nieuwenhuys, J. Catal. 199 (2001) 48.
[16] R.J.H. Grisel, J.J. Slyconish, B.E. Nieuwenhuys, Top. Catal. 16/17 (2001) 425.
[17] M.J. Kahlich, H.A. Gasteiger, R.J. Behm, J. Catal. 182 (1999) 430.
[18] A. Goossens, M.W.J. Crajé, A.M. van der Kraan, A. Zwijnenburg, M. Makkee, J.A. Moulijn, R.J.H. Grisel, B.E. Nieuwenhuys, L.J. de Jongh, Hyperfine Interact., submitted for publication.
[19] R.J.H. Grisel, P.J. Kooyman, B.E. Nieuwenhuys, J. Catal. 191 (2000) 430.
[20] Y. Kobayashi, S. Nasu, S. Tsubota, M. Haruta, Hyperfine Interact. 126 (2000) 95.
[21] D.A.H. Cunningham, W. Vogel, M. Haruta, Catal. Lett. 63 (1999) 43.